

Distribution of Distances between Units in Two-Dimensional Excluded-Volume Chains

Ana M. Torres, Ana M. Rubio, and Juan J. Freire*

Departamento de Química Física, Facultad de Ciencias Químicas, Universidad Complutense, 28040 Madrid, Spain

Marvin Bishop

Department of Mathematics and Computer Science, Manhattan College, Riverdale, New York 10471

Julian H. R. Clarke

Department of Chemistry, University of Manchester Institute of Science and Technology, Manchester M60 0QD, U.K.

Received December 12, 1993; Revised Manuscript Received March 9, 1994*

ABSTRACT: The distribution of distances between different pairs of units in a two-dimensional linear flexible polymer chain with net repulsive interactions between units (i.e., in the excluded-volume regime) is investigated through an off-lattice Monte Carlo method. Three different cases, according to the position of the pair components (end or interior units), are studied. The results are in excellent agreement with theoretical predictions generated by Coulomb gas techniques and conformal invariance methods. Some of these results, however, differ clearly from the values obtained in previous simulations or from those predicted by ϵ expansion formulas based on the renormalization group theory.

Introduction

The influence of intramolecular forces on the conformational properties of linear flexible chains is a long-standing problem.¹⁻³ Many of these properties can be characterized through distribution functions of the distances between the different pairs of units, $F(R_{ij})$. Even though the flexible chain can be modeled as a number N of Gaussian subunits, the form of these distributions differs dramatically from Gaussian when intramolecular forces are present. Explicitly, if i and j are separated by a sufficiently high number of other units, one should consider three different asymptotic behaviors: (A) i and j are both end units (rings); (B) i is an end unit and j is an interior unit (tadpoles); (C) i and j are interior units (twin-tailed tadpoles). (See Chart 1). Assuming a purely repulsive intramolecular potential (which well describes the case of an isolated polymer chain immersed in a good solvent, i.e., a chain in which repulsive forces dominate (excluded-volume regime), a Lagrangian theoretical approach established by des Cloizeaux⁴ has been used to arrive at general scaling forms in terms of critical exponents for the above three cases in the short- and long-distance limits. According to Redner,⁵ both limits are consistently reproduced by a single general function, which, properly normalized, can be written⁶ as

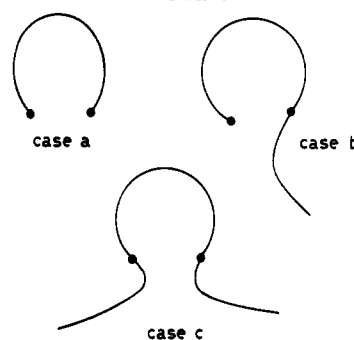
$$F(R_{ij}) = C \langle R_{ij}^2 \rangle^{-d/2} (R_{ij}^2 / \langle R_{ij}^2 \rangle)^{\theta_k/2} \times \exp[-(KR_{ij}^2 / \langle R_{ij}^2 \rangle)^{t/2}] \quad (1)$$

where $\langle R_{ij}^2 \rangle$ is the quadratic mean distance between i and j . The constants involved in eq 1 are

$$K = \{\Gamma[(d+2+\theta_k)/t] / \Gamma[(d+\theta_k)/t]\}^{1/2} \quad (2)$$

* Abstract published in *Advance ACS Abstracts*, May 15, 1994.

Chart 1



case a) rings, b) tadpoles, c) twin-tailed tadpoles

(Γ is the gamma function) and

$$C = tK^{\theta_k+d} / \{\Gamma[(d+\theta_k)/t] (\int_{\Omega} d\Omega)\} \quad (3)$$

where $d\Omega$ represents the angular part of $d\mathbf{r}_{ij}$.

Here d is the space dimension, and the exponent t is expressed in terms of the critical exponent ν as

$$t = 1/(1-\nu) \quad (4)$$

(Therefore, t depends on d .) Finally the exponents θ_k ($k = 0, 1$, or 2) depend on d and also on the case considered (A, B, and C, respectively). These exponents have been evaluated by several theoretical and simulation techniques; for example, the renormalization group second-order expansion in $\epsilon = 4 - d$ provides predictions for these exponents, through the use of summations of Borel transformations.⁴

In a previous paper,⁷ we have verified that the numerical values for θ_0 , θ_1 , and θ_2 obtained through these theoretical methods for 3D ($d = 3$) chains are in good agreement with Monte Carlo results. These calculations used an off-lattice model of Gaussian units subject to Lennard-Jones in-

Table 1. Values of the Exponents θ_k from Theory and Simulations

	conformal theory ^a	ϵ expansion second order ^b			from slopes in Figures 2–4 ^e
		direct	Borel	previous simulations	
θ_0	0.44	0.78	0.61	0.46 ^c	0.44 ± 0.02
θ_1	0.83	0.81	0.85	0.84 ± 0.13, ^d 0.84 ± 0.10 ^e	0.83 ± 0.03
θ_2	1.58	0.12	1.14	1.93 ± 0.27 ^f	1.53 ± 0.07

^a References 4 and 9. ^b From formulas contained in ref 4. ^c Combination of very accurate numerical values for ν and γ from refs 13 and 14; see text. ^d Reference 10. ^e Reference 11. ^f Reference 5. ^g From the $\epsilon/k_B T = 0.1$ points in Figure 4.

tramolecular interactions. The Lennard-Jones parameters were set to describe chains in the excluded-volume regime.

A general description of the scaling forms expected for the three distribution functions is given in ref 8. In the 2D case, ϵ expansions are expected to give poorer results. On the other hand, Duplantier and Saleur⁹ have used Coulomb gas techniques with conformal invariance arguments to predict ν , the different θ_k 's, and other exponents of interest (such as exponent γ , related to the number of configurations) for 2D. These theoretical predictions differ significantly from those derived from the ϵ expansion methods (direct or through Borel summations) for θ_0 and θ_2 . (For θ_2 the different ϵ expansion methods lead to sharply different values.) Previous numerical simulations for the distributions (exact enumeration of conformations in square lattices^{10,11}) reported results in agreement with the theoretical values for θ_1 . Numerical results for θ_2 have also been reported,⁵ but they differ from all the theoretical predictions. Moreover, numerical data for exponents ν and γ , obtained by enumerating self-avoiding chains and polygons,^{12,13} are very close to the predictions of the conformal theory and can be combined as $\theta_0 = (\gamma - 1)/\nu$, yielding a value of θ_0 also in agreement with this theory. (A previous Brownian dynamics study of the end-to-end distribution function¹⁴ did not carry out the explicit evaluation of the exponent θ_0 .) A summary of existing theoretical and simulation values of the different exponents θ_k can be found in Table 1.

In this work, we have performed a Monte Carlo study of the distribution functions $F(R_{ij})$ for two-dimensional chains, with the same off-lattice model that we have previously used for 3D chains. From these functions we have obtained numerical values for θ_0 , θ_1 , and θ_2 . These exponents have been compared with the theoretical predictions. In this way, we have verified the validity of the theoretical methods mentioned above.

Models and Methods

We consider N Gaussian beads of mean length b (b is adopted as the length unit). Nonneighboring beads interact through a 6–12 Lennard-Jones potential. The reduced potential parameters, σ/b and $\epsilon/k_B T$, are set to reproduce the excluded-volume region (as will be justified in the next section). We will also report some calculations made with $\epsilon/k_B T = 0$, i.e., for a chain without intramolecular interactions (unperturbed or non-excluded-volume chain).

Our Monte Carlo algorithm starts by building an initial chain conformation of moderate energy. New conformations are then generated by selecting a bead vector (defined as the vector connecting a bead and its nearest neighbor closest to the chain center) and resampling each of its components from a Gaussian distribution with mean zero and mean-square deviation $b^2/2$. The rest of the chain, up to the end closest to the resampled bead, is rotated and then connected to the new bead. (This sampling can be considered as a form of the pivot algorithm.) Eight different runs are performed (each starts with a different seed number and attempts 60 000 conformations, disregarding 10 000 for thermalization). The uncertainties and means for

Table 2. Dimensions and Scaling Law Exponent Data for Different Chain Lengths and Solvent Conditions

$\epsilon/k_B T$	N	$\langle S^2 \rangle$	$\langle R^2 \rangle$
0.00	55	9.13 ± 0.04	53.6 ± 0.3
	101	16.70 ± 0.06	99.4 ± 0.5
	201	33.5 ± 0.2	200 ± 2
	ν_S, ν_R	0.497 ± 0.002	0.503 ± 0.001
	25	12.18 ± 0.04	84.7 ± 0.3
	37	21.83 ± 0.07	153.9 ± 0.6
0.10	51	35.3 ± 0.1	249 ± 1
	55	39.7 ± 0.3	283 ± 3
	73	61.5 ± 0.2	438 ± 2
	101	97.9 ± 0.6	692 ± 4
	201	257 ± 2	1961 ± 18
	ν_S, ν_R	0.728 ± 0.02	0.740 ± 0.002
0.15	25	12.00 ± 0.03	83.2 ± 0.4
	37	21.40 ± 0.07	150.6 ± 0.8
	51	34.7 ± 0.2	245 ± 2
	73	58.8 ± 0.4	418 ± 3
	ν_S, ν_R	0.722 ± 0.005	0.735 ± 0.02
0.20	25	11.71 ± 0.05	81.0 ± 0.5
	37	20.9 ± 0.1	145.8 ± 0.8
	51	33.2 ± 0.2	233 ± 2
	73	56.9 ± 0.3	402 ± 2
	ν_S, ν_R	0.718 ± 0.003	0.735 ± 0.05
0.25	25	11.29 ± 0.05	77.5 ± 0.3
	37	19.98 ± 0.08	139.2 ± 0.7
	51	32.1 ± 0.2	224 ± 2
	73	54.6 ± 0.3	383 ± 2
	ν_S, ν_R	0.717 ± 0.003	0.727 ± 0.03

averaged quantities such as the mean quadratic radius of gyration, $\langle S^2 \rangle$, or end-to-end distance, $\langle R^2 \rangle$, are estimated by considering every run value as an independent result. We also compute the histogram describing the number of conformations which fall in bins of values of R_{ij} , for each relevant pair of units i and j (only selected pairs symmetrically displaced from the chain center are considered). The functions $F(R_{ij})$ are calculated from these histograms, through a normalization which takes into account the total number of conformations and the surface corresponding to the chosen grid interval. A number of different grid intervals have been examined, in order to choose an optimal value which will provide the highest possible number of intervals compatible with reasonably smooth distribution functions.

Results and Discussion

In Table 2, we present a summary of our results for the averages and deviations of the mean of $\langle S^2 \rangle$ and $\langle R^2 \rangle$, for the unperturbed chains, i.e., obtained with $\epsilon/k_B T = 0$, and for excluded-volume chains with $\epsilon/k_B T = 0.1$ ($\sigma/b = 0.8$). These parameters have been previously shown^{7,15,16} to reproduce the correct critical exponent ν for three-dimensional excluded-volume chains, from consideration of mean size vs chain length scaling law fittings. Following the same procedure for 2D chains, we have used the results contained in Table 2 to perform log–log fits to the equations

$$\langle S^2 \rangle \sim N^{2\nu_S} \quad (5)$$

and

$$\langle R^2 \rangle \sim N^{2\nu_R} \quad (6)$$

The fitted values of ν_S and ν_R for the unperturbed and excluded-volume chains, contained in Table 2, are in good agreement with the exponents predicted^{3,4} by theory for 2D chains, $\nu_S = \nu_R = 1/2$ or $3/4$, respectively, and also with the numerical results reported in our previous study of dimensions for 2D linear and star chains. This study

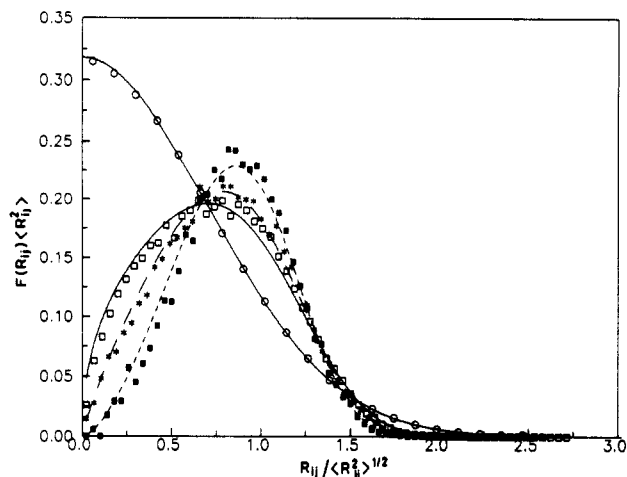


Figure 1. Scaled end-to-end distance distribution function $F(R_{ij})\langle R_{ij}^2 \rangle$ vs $R_{ij}/\langle R^2 \rangle^{1/2}$ in cases A (\square), B ($*$), and C (\blacksquare) for EV chains ($\epsilon/k_B T = 0.1$) with $|i - j| = 72$ ($N = 145$ for cases B and C). The theoretical curves (solid for case A, long dash for case B, and short dash for case C) are obtained from eqs 1–4 with θ_k according to the conformal theory values (see text). (\circ) Results for case A obtained with an unperturbed chain, $N = 101$ together with a solid line corresponding to the Gaussian function for 2D chains.

employed the same chain model and Monte Carlo algorithm but used different statistical samples.¹⁷

The values of averaged dimensions obtained for some higher values of $\epsilon/k_B T$ used in the characterization of the present model Θ state¹⁸ are also shown in Table 2. The values shown here are, however, low enough to reproduce the asymptotic behavior of global properties in the good solvent regime for the present values of N , as can be verified from the fitted numerical values of ν_S and ν_R , also included there and only slightly smaller than the theoretical limit in all cases.

In Figure 1, we show results for the $F(R_{ij})$ functions corresponding to the three cases of interest, A, B, and C. The data have been calculated with $\epsilon/k_B T = 0.1$. According to the arguments given in the previous paragraph, this value cannot be consequently considered as a fitted parameter that reproduces the expected results but a choice for which the asymptotic good solvent behavior has been clearly built up. The results were obtained with $|i - j| = 73$ (in a chain of 145 beads for cases B and C). The end-to-end distance distribution function obtained with the unperturbed chain of $N = 101$ units is also included in the figure. The remarkable influence of excluded-volume effects on the shape of the distribution functions can easily be observed and, also, the distinction among the shapes associated with the A, B, and C cases. (The differences are considerably clearer than for three-dimensional chains.) The theoretical curves for the excluded-volume chains, obtained according to eqs 1–4, with the values of θ_0 , θ_1 , and θ_2 provided by the conformal invariance method⁹ are plotted for comparison, as well as the distribution function for Gaussian 2D chains.² The agreement between all the Monte Carlo results and the corresponding theoretical predictions is excellent. (We have computed also results for smaller values of $|i - j|$. As in our previous study of three-dimensional chains with excluded volume, the agreement with theoretical curves is better as $|i - j|$ increases, provided that the total chain length is high enough.)

We have also carried out a more careful analysis of the distribution functions in the small R_{ij} limit, in order to obtain numerically fitted values of the exponents that can be compared with the theoretical predictions. Thus, we

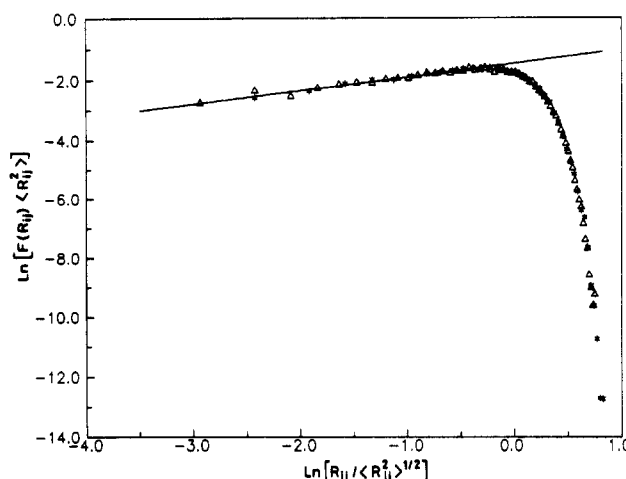


Figure 2. ln–ln plot of $F(R_{ij})\langle R_{ij}^2 \rangle$ vs $R_{ij}/\langle R^2 \rangle^{1/2}$ for the results corresponding to case B for chains with $N = 51$ units (Δ) and $N = 101$ units ($*$). Solid line: Linear fit of the low R_{ij} range.

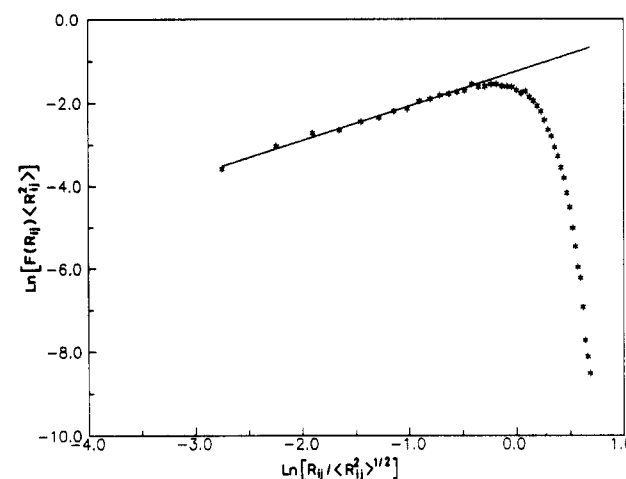


Figure 3. ln–ln plot of $F(R_{ij})\langle R_{ij}^2 \rangle$ vs $R_{ij}/\langle R^2 \rangle^{1/2}$ for the results corresponding to case B in Figure 1 ($*$). Solid line: Linear fit of the low R_{ij} range.

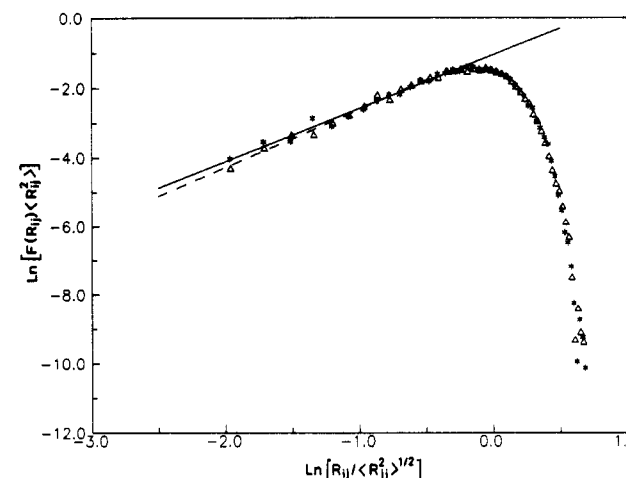


Figure 4. ln–ln plot of $F(R_{ij})\langle R_{ij}^2 \rangle$ vs $R_{ij}/\langle R^2 \rangle^{1/2}$ for the results corresponding to case C in Figure 1 ($*$). Solid line: Linear fit of the low R_{ij} range. Results obtained with $\epsilon/k_B T = 0.15$ are also shown (Δ), together with their linear fit in the low R_{ij} range (dashed line).

present in Figures 2–4 our numerical values of $F(R_{ij})$ for cases A, B, and C, in ln–ln plots. These plots have been used previously^{7,19} in similar analyses for 3D chains. According to eq 1, the linearly fitted slopes of the ln–ln plots at low R_{ij} yield direct estimates of the θ_k exponents. These fitted values are contained in Table 1. They are in very good agreement with the Duplantier and Saleur

(conformal invariance) calculations^{8,9} and differ significantly from the results obtained through ϵ expansion approaches^{4,8} for θ_0 and θ_2 . Moreover, they agree with other numerical data previously reported^{10,11} for θ_1 and with the value of θ_0 that can be obtained by combining existing numerical results^{12,13} for critical exponents γ and ν . Nevertheless, they differ significantly from a previous simulation value⁵ for θ_2 . (See Table 1 for a more complete comparison with the different theory and simulation data.) The agreement with the conformal theory (which is exact in two dimensions) serves, on the other hand, to confirm the validity of the small R_{ij} analysis used to obtain numerical values of θ_k . (We have previously⁷ applied this method to the 3D case, for which exact theory is not available.)

In Figure 4, we also include data obtained with $\epsilon/k_B T = 0.15$. These results show essentially the same scaling form as those calculated with $\epsilon/k_B T = 0.1$. Thus, the slope in the low R_{ij} range obtained with $\epsilon/k_B T = 0.15$ and $\theta_2 = 1.66 \pm 0.06$ is only slightly higher than the one calculated from the $\epsilon/k_B T = 0.1$, included in Table 1 (with overlapping error intervals). This confirms that both sets of results closely follow the good solvent asymptotic behavior of the present model, in spite of the 50% difference for their respective values of $\epsilon/k_B T$.

In summary, our 2D off-lattice Monte Carlo results for the distribution functions of distances between units, of different types, $F(R_{ij})$ in excluded-volume chains, are in good quantitative agreement with the normalized theoretical des Cloizeaux–Redner scaling forms. These forms involve the numerical exponents θ_k , derived by conformal invariance methods for each of the types (rings, tadpoles, or twin-tailed tadpoles).

Acknowledgment. This research has been supported by Grant No. PB92-0227 of the DGICYT (Spain), the NATO Collaborative Research Grants Programme (Grant No. CRG 911005), and the donors of the Petroleum Research Fund, administered by the American Chemical Society.

References and Notes

- (1) Flory, P. J. *Principles in Polymer Physics*; Cornell University Press: Ithaca, NY, 1953.
- (2) Yamakawa, H. *Modern Theory of Polymer Solutions*; Harper and Row: New York, 1971.
- (3) de Gennes, P.-G. *Scaling Concepts in Polymer Physics*; Cornell University Press: Ithaca, NY, 1979.
- (4) des Cloizeaux, J. *J. Phys.* **1980**, *41*, 223.
- (5) Redner, S. *J. Phys. A* **1980**, *13*, 3525.
- (6) Bishop, M.; Clarke, J. H. R.; Rey, A.; Freire, J. J. *J. Chem. Phys.* **1991**, *95*, 4589. Rey, A.; Freire, J. J.; García de la Torre, J. *Polymer* **1991**, *33*, 3477.
- (7) Rubio, A. M.; Freire, J. J.; Bishop, M.; Clarke, J. H. R. *Macromolecules* **1993**, *26*, 4018.
- (8) des Cloizeaux, J.; Jannink, G. *Polymers in Solution. Their Modelling and Structure*; Clarendon Press: Oxford, U.K., 1990.
- (9) Duplantier, B.; Saleur, H. *Phys. Rev. Lett.* **1987**, *59*, 539.
- (10) Guttman, A. J.; Sykes, M. F. *J. Phys.* **1973**, *C6*, 945.
- (11) Trueman, R. E.; Whittington, S. G. *J. Phys.* **1972**, *A5*, 1664.
- (12) Enting, I. G.; Guttman, A. J. *J. Phys. A* **1985**, *18*, 1007.
- (13) Guttman, I. J. *J. Phys. A* **1987**, *20*, 1839.
- (14) Bishop, M.; Clarke, J. H. R. *J. Chem. Phys.* **1989**, *91*, 6345.
- (15) Freire, J. J.; Rey, A.; García de la Torre, J. *Macromolecules* **1987**, *20*, 342.
- (16) Freire, J. J.; Rey, A.; Bishop, M.; Clarke, J. H. R. *Macromolecules* **1991**, *24*, 6494.
- (17) Bishop, M.; Clarke, J. H. R.; Rey, A.; Freire, J. J. *J. Chem. Phys.* **1991**, *95*, 608.
- (18) Torres, A.; Rubio, A. M.; Freire, J. J.; Bishop, M.; Clarke, J. H. R. *J. Chem. Phys.*, in press.
- (19) Baumgärtner, A. *Z. Phys. B* **1981**, *42*, 265.